Nano-Brass: Bimetallic Copper/Zinc Colloids by a Nonaqueous Organometallic Route Using $[Cu(OCH(Me)CH_2NMe_2)_2]$ and Et_2Zn as Precursors

Julia Hambrock, Marie K. Schröter, Alexander Birkner, Christoph Wöll, and Roland A. Fischer*

Lehrstuhl für Anorganische Chemie II, Organometallics & Materials Chemistry, Ruhr-University Bochum, D-44780 Bochum, Germany

Received March 10, 2003. Revised Manuscript Received July 31, 2003

We present a synthetic approach toward alloyed Cu/Zn nanoparticles using $[Cu(OCH(Me)CH_2NMe_2)_2]$ and Et_2Zn as precursors. The thermolysis in the hot coordinating solvent hexadecylamine, HDA, leads to the formation of nanoscale, colloidal Cu/Zn systems with zinc contents (by EDX) of 5, 30, and 65%, respectively. All systems have been analyzed using UV/Vis spectroscopy, transmission electron microscopy, EDX, and selected area electron diffraction (SAED). These analytical data suggest that alloying between zinc and copper takes place, revealing crystalline phases of CuZn and $CuZn_2$ besides Cu as components of the particles in the case of higher zinc concentrations. The characteristic surface plasmon resonance (UV) for pure HDA-capped copper colloids at 558 nm, still observed for copper-rich alloy particles, disappears for zinc-rich particles.

Indroduction

Many heterogeneous catalysts can be regarded as nanocomposites of high surface area metal nanoparticles dispersed on suitable support materials, and the catalyst is promoted by various additives. Among those systems, the Cu/ZnO nanocomposite is prototypical for the so-called strong metal−support interaction (SMSI) and of particular importance for the large-scale industrial methanol production from syngas at moderate temperatures and pressures.[1−3] Such copper-based methanol catalysts can be grouped into three classes: the binary systems Cu/ZnO and Cu/Al_2O_3 and the ternary system $Cu/ZnO/Al_2O_3$. These catalysts are prepared along precisely controlled aqueous coprecipitation/calcination/reduction procedures using cheap copper and zinc salts (nitrates, carbonates, and acetates) as precursors. The catalytically active systems show a linear correlation of the methanol productivity with the specific copper surface.[4,5] It is known that the Al_2O_3 component stabilizes the system against sintering (structural promotor) and the ZnO component further increases the activity at a given copper dispersion. Much research has been directed to elucidate the special nature of the synergetic effect between the Cu and the ZnO component. Most recent studies revealed that the structure of local sites at the Cu/ZnO interface seem to be most important and relate to the segregation of Zn species to the Cu surfaces, forming a Cu/Zn surface alloy as well as surface Zn atoms and ZnO ad-species as a function of the redox potential of the ambient (composition of the gas and temperature/pressure). Consequently, the state of the catalyst appears to be dynamic, and different types of structures may only be dominant features under limited sets of reaction conditions as some leading authors in that field have pointed out.[6,7]

We were attracted by the relevance and complexity of the Cu/ZnO nanocomposite in the solid state and started out to establish a colloidal chemistry of the Cu/ZnO system with the long-term goal of deriving some type of soluble model catalyst to enter the above cited discussion from a new side. There exists a plethora of work on copper colloids and ZnO colloids for many reasons referring to fundamental interests, for example, effects of particle size, shape, and surface structure on physical properties, "size quantization", along the transition from the bulk to molecular dimensions and thus addressing many interesting applications.[8−16] However,

* To whom correspondence should be addressed. E-mail: Roland.Fischer@ruhr-uni-bochum.de.

(1) Hansen, J. B. *Handbook of Heterogeneous Catalysis, Vol. 4*; Wiley-VCH: New York, 1997.
(2) Klier, K. *Adv. Catal.* **1992**, *31*, 243.
(3) Waugh, K. C. *Catal. Today* **1992**, *15*, 51.
(4) Kurtz, M.; Wilmer, H.; Genger, T.; Hinrichsen, O.; Muhler, M. *Catal. Lett.* **2003**, *86*, 77−80.
(5) Bauer, N.; Büscher, C.; Kutz, M.; Wilmer, H.; Hirichsen, O.; Becker, R.; Rabe, S.; Merz, K.; Fischer, R.; Driess, M.; Muhler, M. *Abstract for the XXXVI. Annual Meeting Deutscher Katalytiker*, Weimar, 2003.
(6) Greeley, J.; Gokhale, A. A.; Kreuser, J.; Dumesic, J. A.; Topsoe, H.; Topsoe, N.-Y.; Mavrikakis, M. *J. Catal.* **2003**, *213*, 63.
(7) Hansen, P. L.; Wagner, J. B.; Helveg, S.; Rostrup-Nielsen, S. R.; Clausen, B. S.; Topsoe, H. *Science* **2002**, *295*, 2053.
(8) Pileni, M. P. *J. Am. Chem. Soc.* **1993**, *115*, 3887.
(9) Lisiecki, I.; Billoudet, F.; Pileni, M. P. *J. Phys. Chem.* **1996**, *100*, 4160.
(10) Ayyappan, S.; Gopalan, R. S.; Subbanna, G. N.; Rao, C. N. R. *J. Mater. Res.* **1997**, *12* (2), 398.
(11) Huang, H. H.; Yan, F. Q.; Kek, Y. M.; Chew, C. H.; Xu, G. Q.; Ji, W.; Oh, P. S.; Tang, S. H. *Langmuir* **1997**, *13*, 172.
(12) Koch, U.; Fojtik, A.; Weller, H.; Henglein, A. *Chem. Phys. Lett.* **1985**, *122*, 507.
(13) Bahnemann, D. W.; Kormann, C.; Hoffmann, M. R. *J. Phys. Chem.* **1987**, *91*, 3789.
(14) Spanhel, L.; Andersen, M. A. *J. Am. Chem. Soc.* **1991**, *113*, 2826.

10.1021/cm0341383 CCC: $25.00
Published on Web 10/09/2003

almost nothing is known about Cu/ZnO colloids, that is, free-standing, surface-stabilized, and soluble Cu-decorated ZnO nanoparticles or vice versa, ZnO_x-decorated Cu particles, which would represent one kind of a soluble catalyst model. On the other hand, we could not find anything about bimetallic free-standing Cu/Zn alloy nanoparticles dispersed in colloidal solution. There does exist a wealth of literature on other bimetallic nanocolloids typically containing noble metals including Ag/Au,[17] Ag/Pd,[18] Au/Pd,[18,19] Au/Pt,[20] Pd/Cu,[21] and Pt/Ru[22] with applications in heterogeneous/homogeneous catalysis and also Fe/Pt,[23,24] Co/Pt,[25−27] and Ni/Pd[28] colloids containing mixtures of the ferromagnetic iron-group metals with platinum-group metals, for example, having potential use as magnetic nanoalloys in future information storage systems.[23,29,30] But up to now, it seems that there has not been a motivation to study the nano-chemistry and -physics of the collodial Cu/Zn system. On the basis of our previous work on nonaqueous colloids (NACs) of copper particles, stabilized by HDA (*h*exa*d*ecyl*a*mine) in toluene, which were derived from thermolysis of the metallo-organic precursor [Cu{$OCH(Me)CH_2NMe_2$}$_2$] (**1**) in pure hexadecylamine (HDA),[31] we now wish to present our new results on the synthesis and characterization of Cu/Zn−NACs, that is, "nano-brass", using **1** and diethylzinc as precursors for copper and zinc, respectively.

Materials and Methods

Et_2Zn (Strem), hexadecylamine (Acros), and *n*-octylamine (Acros) were commercially available. Et_2Zn was used without further purification, HDA was dried at 100 °C by repeatedly applying vacuum over 30 min, and *n*-octylamine was dried, distilled, and degassed prior to use.

[$Cu(OCH(Me)CH_2NMe_2)_2$] (**1**) was prepared as described by Buhro and co-workers,[32] by reacting copper methanolate with the corresponding amino alcohol in an alcohol-exchange procedure.

The solvents used for preparation and workup procedures were dried, distilled, and stored under argon. In addition, the solvents used for the workup procedure were also degassed.

UV/Vis Spectroscopy. A Perkin-Elmer Lambda 9 UV/VIS/NIR spectrophotometer was used to carry out the optical measurements. Samples were dissolved in toluene and were placed in special optical glass cuvettes (1-cm path length).

Electron Microscopy. An Hitachi H-8100 scanning and transmission electron microscope operating at accelerating voltages up to 200 keV with a single-crystal LaB_6 filament was used for the TEM studies. X-ray energy-dispersive spectra (EDS) were obtained from an attached EDX system (Oxford Link with Si(Li) crystal and ultrathin window ATW2). The specimens were prepared by placing a drop of a dilute solution of a sample in toluene on a carbon-coated gold grid and allowed to dry at room temperature.

Method for Preparation of Colloidal Metal Particles. *General*. A sample of 7 g of HDA was dried and degassed by heating to about 100 °C in vacuo. The temperature was then stabilized at 250 °C under about 1 atm of argon. After injection of the precursors, the solution was kept at that temperature for 30 min (note that it temporarily drops to lower temperatures due to the injection of cold reactants). After rapid cooling to room temperature, an excess of dry methanol was added to precipitate the nanocrystals. The particles were washed several times with methanol, centrifuged from the supernatant, and then redissolved in toluene. All samples (except the 100% zinc particles) were soluble in toluene. **Cu/Zn 100/0**: For the preparation of pure copper particles a sample of 324 mg (1.2 mmol) of **1** (dissolved into 4 mL of *n*-octylamine, see our previous publication) was used.[31] **Cu/Zn 0/100**: For the preparation of the 100% zinc system samples of 15, 150, and 500 mg of Et_2Zn were dissolved in 4 mL of octylamine and then injected into the HAD, all giving the very same results in terms of particle morphology. **Cu/Zn 95/5**: The mixed Cu/Zn system with the lowest zinc content, that is, Cu/Zn 95/5, was obtained by first synthesizing copper nanoparticles as described above, but without workup, and then heating the reaction mixture to about 180 °C (oil bath). A sample of 15 mg of Et_2Zn (0.12 mmol, corresponding to a concentration ratio of the precursors Cu:Zn = 90:10) was dissolved in 4 mL of octylamine and the solution was added dropwise into the hot solution of the copper nanoparticles. The reaction mixture was kept at 180 °C for 10 min and then cooled to room temperature. ***Cu/Zn 70/30***. For this system 147 mg of Et_2Zn (1.2 mmol, corresponding to Cu:Zn = 50:50) were dissolved in 4 mL of octylamine. The synthesis was carried out by injection of this solution into *n*-hexadecylamine as described above. ***Cu/Zn 35/65***: The zinc-rich system was prepared in the same way as the 70/30 system, again using 324 mg of **1** (1.2 mmol) and 500 mg of Et_2Zn (4.0 mmol, corresponding to Cu:Zn = 30:70). It can be prepared similarly to the 95/5 system, too, by first synthesizing copper nanoparticles, including a growth time of 30 min, and then, without cooling, dropwise adding Et_2Zn into this solution. We observed no difference in the SAED pattern as well as the morphology of these particles compared to the first mentioned method, thus ensuring that the two methods can be used alternatively.

Results and Discussion

The synthetic basis for the Cu/Zn systems was a reliable method for the preparation of metallic copper nanoparticles[31] that has recently been published by our group. Shortly, the injection of the Cu(II) precursor [Cu($OCH(Me)CH_2NMe_2)_2$] into a hot coordinating solvent without using further additives yields highly monodisperse, almost spheric, Cu(0) nanoparticles that are covered by long-chain amines, that is, *n*-hexadecylamine (HDA). The particle morphology did not change upon a variation of the concentration of **1** by a factor of 1−100. For reasons of comparison the UV/Vis absorption spectrum as well as the TEM and SAED images of such a

(15) Meulenkamp, E. A. *J. Phys. Chem. B* **1998**, *102*, 5566.
(16) Zhou, H.; Alves, H.; Hofmann, D. M.; Kriegseis, W.; Meyer, B. K.; Kaczmarczyk, G.; Hoffmann, A. *Appl. Phys. Lett.* **2002**, *80*, 210.
(17) Link, S.; Wang, Z. L.; El-Sayed, M. A. *J. Phys. Chem. B* **1999**, *103*, 3529.
(18) Chen, Y.-H.; Tseng, Y.-H.; Yeh, C.-S. *J. Mater. Chem.* **2002**, *12*, 1419.
(19) Wu, M. L.; Chen, D.-H.; Huang, T.-C. *Langmuir* **2001**, *17*, 3877.
(20) Henglein, A. *J. Phys. Chem. B* **2000**, *104*, 2201.
(21) Bradley, J. S.; Hill, E. W.; Chaudret, B.; Duteil, A. *Langmuir* **1995**, *11* (3), 693.
(22) Pan, C.; Dassenoy, F.; Casanove, M.-J.; Philippot, K.; Amiens, C.; Lecante, P.; Mosset, A.; Chaudret, B. *J. Phys. Chem. B* **1999**, *103*, 10098.
(23) Sun, S.; Murray, C. B.; Weller, D.; Folks, L.; Moser, A. *Science* **2000**, *287*, 1989.
(24) Dai, Z. R.; Sun, S.; Wang, Z. L. *Nano Lett.* **2001**, *1* (8), 443.
(25) Ould Ely, T.; Pan, C.; Amiens, C.; Chaudret, B.; Dessanoy, F.; Lecante, P.; Casanove, M.-J.; Mosset, A.; Respaud, M.; Broto, J.-M. *J. Phys. Chem. B* **2000**, *104*, 695.
(26) Park, J.-I.; Cheon, J. *J. Am. Chem. Soc.* **2001**, *123*, 5743.
(27) Carpenter, E. E.; Seip, C. T.; O'Connor, C. J. *J. Appl. Phys.* **1999**, *85*, 5184.
(28) Teranishi, T.; Miyake, M. *Chem. Mater.* **1999**, *11*, 3414.
(29) Weller, H.; Moser, A. *IEEE Trans. Magn.* **1999**, *35*, 4423.
(30) Christodoulides, J. A.; Huang, Y.; Zhang, Y.; Jadjipanayis, G. C.; Panagiotopoulos, I.; Niarchos, D. *J. Appl. Phys.* **2000**, *87*, 6938.
(31) Hambrock, J.; Becker, R.; Birkner, A.; Weiss, J.; Fischer, R. A. *Chem. Commun.* **2002**, *68*.
(32) Goel, S. C.; Kramer, K. S.; Chiang, M. Y.; Buhro, W. E. *Polyhedron* **1990**, *9*, 611.

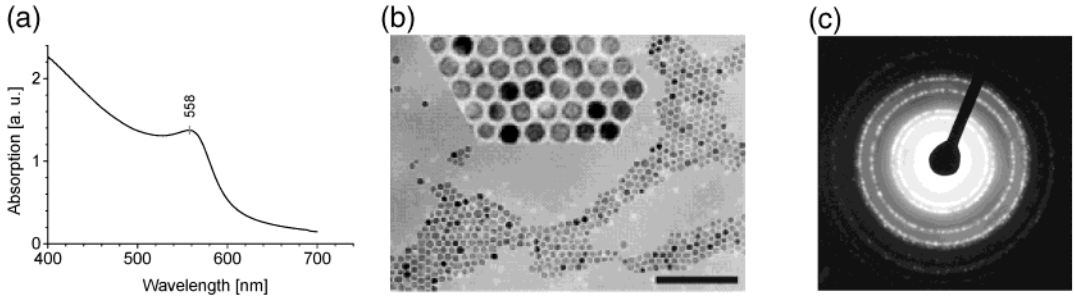

Figure 1. (a) UV/Vis absorption spectrum, (b) TEM image (bar = 110 nm), and (c) SAED of the toluene solution of the **Cu/Zn = 100/0** system.

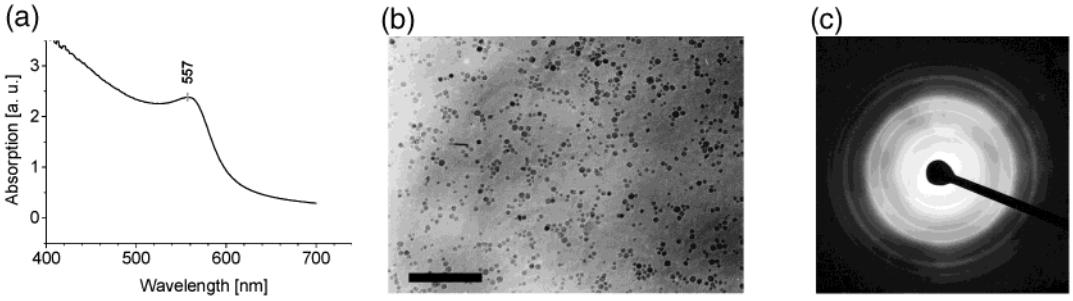

Figure 2. (a) UV/Vis absorption spectrum, (b) TEM image (bar = 175 nm), and (c) SAED of the toluene solution of the **Cu/Zn 95/5** system.

sample, denoted as Cu/Zn 100/0, are shown in Figure 1. The following synthetic procedures for the Cu/Zn systems have been used on condition that [Cu(OCH(Me)CH_2NMe_2)$_2$] was employed as the copper source, HDA as the reaction medium, and octylamine as cosolvent.

Et_2Zn was chosen as the source for elemental zinc. To test its suitability to release zinc after injection into hot HDA, we injected solutions of Et_2Zn in *n*-octylamine of different concentrations into the same amount of hot HDA. Gray precipitates were formed, centrifuged from the supernatant, and washed with methanol. In contrast to the copper nanoparticles, the deposited materials were insoluble in toluene. The TEM images showed wires in the micrometer range, explaining therewith the observed insolubility due to the large dimensions of the material (see Figure 5). We did not observe a change in morphology within the range of the reported concentrations; however, we did not attempt to elucidate this issue in further detail. X-ray diffraction (XRD) confirmed the formation of elemental zinc with the result that Et_2Zn is in fact qualified for the release of Zn(0) upon thermolysis in hot HDA, and thus matching the temperature window for the preparation of the copper particles using **1** as precursor.

For the evaluation of the Cu/Zn alloying system we chose three different Cu/Zn molar ratios of the precursors, that is, 90:10, 50:50, and 30:70. Please note that the final content of copper and zinc of the Cu/Zn particles is slightly different from that of the initial molar ratios: **Cu/Zn 95/5**, **Cu/Zn 70/30**, and **Cu/Zn 35/65** were found by EDX analysis (see below). The reason for this observation is not quite clear. Perhaps, the efficiency of the thermolysis is lower for the less reducable Zn precursor as compared with the copper precursor. However, the deviation is less for higher amounts of the Zn precursor and thus some unintentional hydrolysis/oxidation upon preparation, handling, and injection of the stock solutions of low zinc concentrations must be considered also. After workup (see Materials and Methods section) the resulting HDA-stabilized particles were all soluble in toluene and were characterized by UV/Vis spectroscopy, TEM, EDX, and SAED.

UV/Vis Spectroscopy. Pure, colloidal metallic copper nanoparticles display a distinct surface plasmon resonance (SPR) that is responsible for the intense red color of the solutions. Bulk copper does not exhibit this feature because the fraction of surface electrons is very small compared to the bulk electrons, but for nanoscale material the surface area cannot be neglected any more. Since the absorption wavelength of the SPR is independent from the size of the particles, at least up to a size of about 25 nm, its occurrence and position is a characteristic feature for small nanoparticles. The UV/Vis absorption spectrum of the HDA-stabilized pure copper nanoparticles is shown in Figure 1a and displays a sharp absorption peak at $\lambda = 558$ nm. The position of the SPR is different from the value of our first report (566 nm) when we used samples that contained a large *excess* of *n*-hexadecylamine.[31] Copper nanoparticles that have been precipitated from the synthesis solution and were repeatedly washed with methanol reproducibly exhibit an absorption band at $\lambda = 558$ nm in toluene solution. All samples discussed in this work have been worked up in the same way.

The UV/Vis spectrum of the system **Cu/Zn 95/5** containing 5 mol % (by EDX) of zinc is displayed in Figure 2a. The (local) absorption maximum is located at a wavelength of 558 nm, that is, at the very same value as the pure copper particles. Apparently, a low content of zinc atoms does not affect the surface properties of the Cu/Zn alloy nanoparticles. Of course, there is another explanation, that is to say the coexistence of individual pure Cu and pure Zn particles. Our TEM/EDX equipment did not allow the focusing on individual particles so we are talking about averaged information

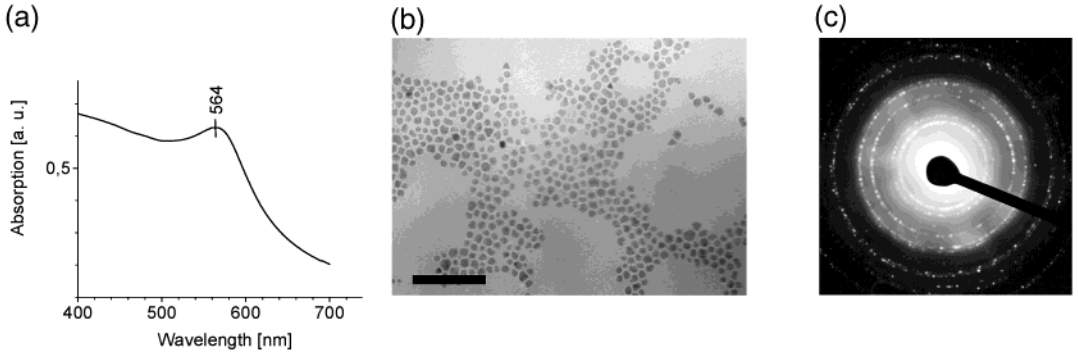

Figure 3. (a) UV/Vis absorption spectrum, (b) TEM image (bar = 116 nm), and (c) SAED of the toluene solution of the **Cu/Zn 70/30** system.

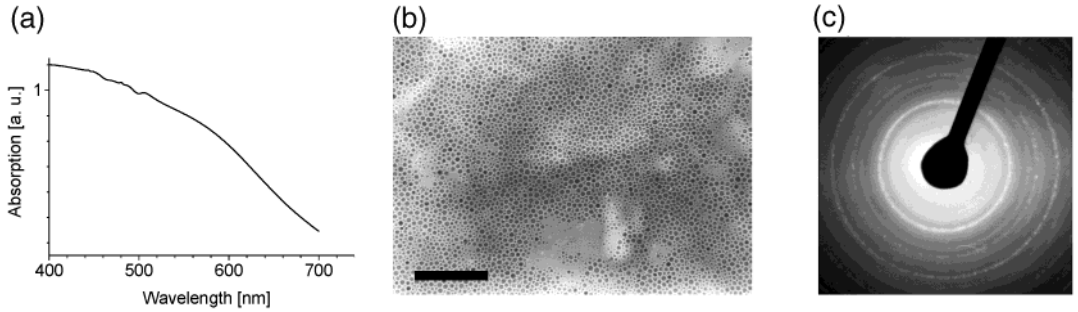

Figure 4. (a) UV/Vis absorption spectrum, (b) TEM image (bar = 184 nm), and (c) SAED of the toluene solution of the **Cu/Zn 35/65** system.

of particle composition. However, a simple coexistence can be excluded by comparison with the data obtained from pure zinc systems: in the case of separate Cu and Zn nanoparticles, the rod-type morphology of zinc particles, being characteristic for our conditions, should appear (see above), which is clearly absent in all of our Cu/Zn samples. Also, the SAED and the chemical behavior referring to oxidation supports the proposed alloying (see below).

If the ratio of copper to zinc is decreased to **Cu/Zn 70/30**, the UV/Vis spectrum of the respective toluene solution displays an absorption band at $\lambda = 564$ nm (Figure 3a). Compared to pure copper nanoparticles, this value is clearly red-shifted. The shift indicates that the SPR of the particles is no longer caused by pure copper, but is interfered by additional effects. Since the ligands (HDA) that coordinate to the surface are the same as those for Cu(0) nanoparticles, it is very reasonable to assign this effect to alloyed zinc present in the particles.

For the zinc-rich sample **Cu/Zn 35/65** no SPR can be observed in the UV/Vis absorption spectrum of the respective toluene solution (see Figure 4a). This suggests that a rather new system has been formed that provides no surface electrons to be excited by the interaction with visible or UV light. Again, please note that the injection of only Et_2Zn into hot HDA yields material which is not redispersable in toluene. This means if Et_2Zn would be thermolyzed into zinc particles without undergoing any (alloying) reaction with the copper atoms or particles present in the solution, it would be separated out by the workup procedure and would thus not interfere with the UV/Vis absorption of the samples above. We conclude that the observed features thus stem from the *mixed* (alloy) Cu/Zn particles and not from *separated* Cu and Zn particles.

Transmission Electron Microsopy (TEM) and Energy-Dispersive X-ray Analysis (EDX). As reported before[31] the 100% copper system **Cu/Zn 100/0** prepared by the thermolysis of $[Cu(OCH(Me)CH_2NMe_2)_2]$ (**1**) forms almost spherical, well-separated, and highly monodisperse nanoparticles as shown in Figure 1b. At the other end, the 100% zinc system **Cu/Zn 0/100** yields material of a completely different morphology. Et_2Zn forms irregular wires with about 1 μm in length and 50 nm in width when thermolyzed in hot HDA (see Figure 5a), irrespective of the employed zinc concentration (see Materials and Methods section).

Figure 2b shows particles of the **Cu/Zn 95/5** system. The individual particles are clearly separated from their neighbors and have a spherical shape with a rather broad size distribution from 5 to 10 nm. The low monodispersity most likely originates from the starting copper nanoparticles, which already had a broad size distribution of the same range in these cases. We did not attempt to optimize the size distribution yet. But this should be possible by careful elucidating the conditions. An EDX analysis performed on the nanoparticles results in a spectrum with peaks for Cu and Zn, confirming that both elements are present. The quantitative analysis of the Kα lines of copper and zinc revealed a molar ratio of Cu:Zn = 95:5. This means that the particles contain less zinc than originally employed (the ratio of precursors was Cu:Zn = 90:10). A possible explanation is the formation of low molecular weight (molecular) Zn-containing side products (e.g., hydrolysis), which are separated out by the precipitation/washing procedure (see above).

For a higher content of zinc **Cu/Zn 70/30** we observe a similar morphology as shown in Figure 3b. The particles have a spherical shape with a mean diameter of about 10 nm and are still separated from each other.

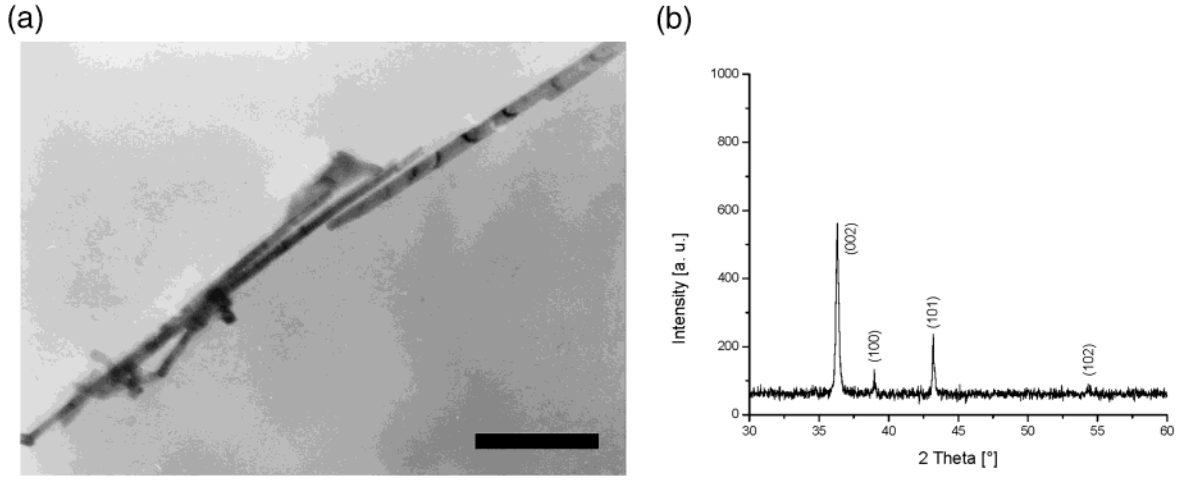

Figure 5. (a) TEM image (bar = 500 nm) and (b) powder XRD of the **Cu/Zn = 0/100** system.

Table 1. Observed Lattice Distances and Reference Data (JCPDS)[a]

100/0	95/5	70/30	35/65	copper	zinc	zinc oxide	Cu_5Zn_8	brass	CuZn[#]	$CuZn_2$[§]
						2.81 (57)				
						2.60 (44)				
			diffuse		2.47 (53)	2.48 (100)				
		2.35	signals (b)		2.31 (40)					2.35 (50)
										2.16 (40)
2.09	**2.09**	**2.10**	**2.09** (b)	2.09 (100)	2.09 (100)		2.09 (100)	2.12 (100)	2.09 (100)	2.08 (100)
						1.91 (23)		2.06 (17)		
1.81	**1.80**	**1.80**	1.82	1.81 (46)				1.83 (35)		
					1.69 (28)					
		1.61	1.63			1.62 (32)				1.59 (30)
			1.48			1.48 (29)			1.47 (15)	
		1.37	1.38			1.38 (23)				1.37 (40)
					1.34 (25)					
					1.33 (21)					
1.28	**1.28**	**1.27**	1.28	1.28 (20)						
		1.21	**1.21**				1.21 (10)		1.20 (29)	1.23 (30)
		1.16								1.16 (30)
1.09	**1.09**	**1.10**	1.10	1.09 (17)						

[a] The *d* spacings are given in Å; the numbers in brackets represent the relative intensities of the respective reflections. For the reference phases only those reflections with relative intensities of $I > 5$ (for $CuZn_2$ $I > 10$) are given ([#]Zhanghengite, [§]Danbaite). Broad and diffuse reflections are denoted as (b). Bold numbers refer to the observed reflections of dominant intensity.

However, they are more faceted than those with a lower content of zinc, the size distribution is broader, and a small fraction shows a triangular shape. Here, too, the amount of zinc that was determined by EDX analysis is smaller than what could be expected from the ratio Cu/Zn in the synthetic procedure (a 1:1 molar ratio of Cu/Zn was used for injection).

The sample **Cu/Zn 35/65** reveals spheres such as the 70/30, 95/5, and 100/0 systems as can be seen in Figure 4b. These particles have a size of about 10 nm and are well-separated, as expected. The composition was determined by means of EDX analysis.

Diffraction (SAED and XRD) and Stability against Oxidation. The selected area electron diffraction (SAED) of pure copper nanoparticles is shown in Figure 1c. The sample has been prepared and transferred to the TEM in an inert gas atmosphere using an Ar-filled drybox and a vacuum transfer holder. The diffraction pattern clearly shows reflection spots and circles that can be assigned to the (111), (200), (220), and (331) lattice planes of the cubic phase of copper. We found that these samples easily oxidize within minutes when allowed to have contact with air, resulting in two additional rings that match the reflections of CuO and Cu_2O, respectively. We believe that only the surface is oxidized upon contact with air because (1) the intense and definite copper reflections remain whereas the additional peaks appear weak and diffuse and (2) the oxide reflections are observed for larger particles, too, but their intensity is smaller in accordance with the decreasing surface-to-volume ratio. Thus, we exclude the formation of isolated, free-standing fully oxidized CuO/Cu_2O particles. We rather suggest core−shell particles with an (partially) oxidized shell and a copper metal core.

The presence of 5% zinc results in the SAED pattern shown in Figure 2c. The lattice distances that correspond to the reflection rings are given in Table 1 and again can be assigned to the (111), (200), (220), and (331) lattice planes of metallic copper. Although we exposed the sample to air after the preparation in a drybox for a couple of minutes, we surprisingly did not observe reflections for copper oxides as in the case of the pure copper particles above. We propose that only the surface is oxidized rather than the whole particle (see above). The oxidation of the copper is suppressed in a system that contains even such a small amount of zinc. The assignment of only copper in the diffraction pattern of the **Cu/Zn 95/5** system fits very well with the observation that the SPR in the UV/Vis absorption spectrum

did not shift compared to that of the pure **Cu/Zn 100/0** system. We thus speculate that some of the zinc content of the particles may segregate to the surface and react with ZnO there if oxygen is present, leading to a rather disordered ZnO or $CuZnO_x$ shell not being detectable by SAED. Clearly, this issue needs further substantiation and more analytical characterization (e.g., by EXAFS), which is currently underway.

At first glance, the number and intensity of the reflections of **Cu/Zn 70/30** (Figure 3c) suggest the presence of metallic Cu without reflections for copper oxides. A closer look, however, reveals that five additional somewhat diffuse rings with low intensity are visible, that is, at *d* spacings of 2.35, 1.61, 1.37, 1.21, and 1.16 Å, respectively. By comparison with the literature data the presence of aggregated (crystalline) zinc or zinc oxide is not very likely because at least two important reflections are missing (see Table 1). The lattice distances of several Cu/Zn alloys are given in Table 1, but only the reflections of $CuZn_2$, danbaite, coincide with the data from SAED. However, the reflection at $d = 2.16$ Å is missing. It is thus suggested that the majority of the nanocrystals are made up of elemental copper with an additional alloy Cu/Zn phase, probably $CuZn_2$. Since it is known that the SPR of these particles shift to higher wavelengths and no reflections for Cu_xO have been detected, it may be that $CuZn_2$ is located on the surface of the crystals.

The sample **Cu/Zn 35/65** reveals a completely different SAED pattern. Whereas metallic copper and the Cu/Zn systems with a low content of zinc characteristically display the four very intense reflections of cubic copper, the SAED image shown in Figure 4c exhibits two reflections of high intensity, that is, at 2.09 and 1.21 Å and an additional one with a moderate intensity at 1.48 Å and several weaker peaks (see Table 1). Again, aggregated zinc and zinc oxide phases cannot explain this feature. Alloying of zinc with copper has to be taken into account. The phase Cu_5Zn_8 would fit the observed data because this Cu/Zn phase exhibits only two characteristic reflections with a moderate intensity, that is, at 2.09 and 1.21 Å, which are the features of highest intensity in Figure 4c. However, the relative intensity of the reflection at 1.21 Å of Cu_5Zn_8 is reported to be only 10% as compared with 100% for the 2.09 Å reflection. The intensity of the *observed* reflection of our sample at 1.21 Å appears to be substantially higher; that means, there has to be another contribution. The compound in question may be CuZn, which contributes with 29% relative intensity to the reflection at 1.21 Å and also explains the distinct reflection at 1.47 Å. The weak reflections at 1.82 and 1.28 Å can be assigned to a small amount of crystalline copper metal, whereas the reflections at 1.63 and 1.38 Å most likely stem from $CuZn_2$. Brass may be present as well since all the reflections (2.12, 2.06, and 1.83 Å) are present. Note that due to its broadness the reflex at 2.09 Å may include both the 2.12 and 2.06 Å reflexes. However, since the reflection at 1.82 Å is very weak and has contributions from elemental copper as well, the amount of brass if any is assumed to be small. Because of the experimental limitations and the rather qualitative nature of our data, it is certainly not possible to present an unambiguous assignment of the observed reflections to known Cu/Zn phases; especially the assignment of Cu_5Zn_8 is not clear and this phase may not be present at all. In addition, the coexistence of *minor* fractions of pure zinc cannot completely be ruled out by the SAED data (see also below). Nevertheless, the SAED data of the mixed Cu/Zn samples reveal evidence for alloying, at least based on the diffractions at $d = 1.16$ and 1.21 Å (Table 1).

Conclusion

Using the thermolysis of the organometallic precursors $[Cu\{OCH(Me)CH_2NMe_2\}_2]$ (**1**) and diethyl zinc in hot coordinating solvents, we achieved the synthesis of Cu/Zn alloy nanocolloids with compositions of Cu:Zn = 95:5, 70:30, and 35:65. We found that the surface plasmon resonance is a very good probe for the (surface) composition of copper nanoparticles because it gradually shifts to higher wavelengths with increasing amount of zinc. Only when the amount of zinc is 30% or higher is the formation of crystalline Cu/Zn alloy phases according to the Cu/Zn phase diagram observed by SAED. All Cu/Zn samples reveal free-standing nanoparticles that are well-dispersed and clearly separated from each other. Even for low fractions of zinc, the oxidation of the copper component is inhibited as compared with pure copper colloids, pointing to surface segregation of zinc and formation of a disordered (amorphous) ZnO/$CuZnO_x$ layer on the particle surface, probably protecting further oxidation of the copper core.

Now having access to such alloyed Cu/Zn nanoparticles, stabilized by HDA in toluene solution, we suggest that intimate contact between Cu and ZnO_x, being important for the methanol catalyst system, can be modeled by first "doping" copper with various amounts of zinc and then intentional and careful oxidation. Strictly speaking, we cannot rule out the formation of unintentional oxide species by our recipe and conditions; at least nonagglomerated, noncrystalline ZnO (and/or Cu_xO) may be present to some extent, not being detected by SAED. A perfect exclusion of air and moisture is extremely difficult and certainly not rigorously possible by the wet chemistry we describe here. Working with Et_2Zn always includes some hydrolysis/oxidation and the resulting species may adsorb or interact with the surface of colloidal particles. In fact, the recently obtained preliminary EXAFS data of our samples point to some Zn as well as ZnO species with a very low degree of agglomeration. Thus, with our goal in mind, that is, ZnO-decorated copper particles as potential models for the binary Cu/ZnO catalytic system, a systematic study and characterization of the oxidation (by detailed EFAXS studies) of our Cu/Zn alloy particles stabilized as nonaqueous colloids is certainly warranted.

Acknowledgment. This work was supported by the German Research Foundation (DFG Priority Program 558 on "Metal−Support Interaction in Heterogeneous Catalysis", Projects B2 and A4).

CM0341383